Journal of the Korean Society of Remote Sensing, Vol. 10, No. 2, 1994

Adaptive Reconstruction Of AVHRR NVI Sequential Imagery of Korean Peninsula

Sanghoon Lee* · Kyungsook Kim**

*Department of Industrial Engineering, Kyung Won University
**Division of Global Environmental Information
Systems Engineering Research Institute
Korea Institute of Science and Technology

Abstract

Multitemporal analysis with remotely sensed data is complicated by numerous intervening factors, including atmospheric attenuation and occurrence of clouds that obscure the relationship between ground and satellite observed spectral measurements. A reconstruction system was developed to increase the discrimination capability for imagery that has been modified by residual effects resulting from imperfect sensing of the target and by atmospheric attenuation of the signal. Utilizing temporal information based on an adaptive temporal filter, it recovers missing measurements resulting from cloud cover and sensor noise and enhances the imagery. The temporal filter effectively tracks a systematic trend in remote sensing data by using a polynomial model. The reconstruction system were applied to the AVHRR data collected over Korean Peninsula. The results show that missing measurements are typically recovered successfully and the temporal trend in vegetation change is exposed clearly in the reconstructed series.

I. INTRODUCTION

Temporal studies with remotely sensed measurements are complicated by numerous intervening factors, such as atmospheric attenuation and cloud occurrence. It tends to obscure the relation between ground and satellite observed spectral measurements. During the last decade, a wide range of statistical techniques has been developed for analyzing spectral imagery at single time step. The evolution of space engineering technology

affects the quantity and quality of data collected through remote sensing. It is now possible to contiguously acquire images at short, regular time intervals. However, statistical approaches to multitemporal analysis of sequential imagery remain largely unexplored, and few are designed to preserve the sequence of the observations in the course of the analysis, although the temporal component in the sequence contains abundant, useful information. The analysis for a long sequence of images with high temporal resolution was made by Lee and Crawford [1], in which an adaptive system was developed with a Bayesian restoration filter and a least squares linear estimation filter with an escalator structure. The Lee's algorithms are based on a general statistical model related to digital image processes of remote sensing. This statistical structure may be so general that it causes complexity in computation and memory for large images. In this study, the Lee's algorithms were modified to be effective and efficient for large remotely sensed images. Though the statistical structure is simplified in the modified system, it involves essential characteristics that are shown in remote sensing data.

In multitemporal analysis of sequential imagery, there is a high likelihood that during data acquisition periods the target site corresponding to any given pixel may be covered by clouds, thereby resulting in missing data. The problem of cloud occurrence may be to some extent avoided through the use of image compositing [2], a procedure in which geographically registered data sets that are collected over a sequential period time are compared and the best of a defined measurement is selected to represent the conditions observed during that time period. This simple method which can be easily automated may be quite effective in reducing cloud contamination given sufficiently long composite period. But it is difficult to maintain a reasonable temporal resolution and also produce cloud-free surface measurements. For any given time-composite period, there is no assurance that cloud-free observations were recorded. Using long composite period will mask the subtler surface changes between the scenes. To overcome this problem, cloud-free imagery can be generated without losing temporal resolution in a given period by automatic unsupervised learning in the system through an adaptive temporal prediction.

Of great importance is the need to incorporate temporal variation of the spectral component according to physical properties of targets and atmospheric changes into image processing techniques. Most physical processes in remote sensing data that are observed from land usually exhibit systematic trends in properties over a long time. This type of variation is most apparent in the mean intensity process of the target distribution, which usually dominates the temporal process. If temporal dependency in a sequence of remotely

sensed images results from special cause rather than common cause, a polynomial model can be used to track a trend in the intensity. With the polynomial model, the intensity at the next time step can be predicted with an exponentially weighted criterion so that the estimate reflects more recent variation in the process. The special and common causes describe the systematic nonstationarity of the mean intensity and the random variation about the mean intensity respectively. If the spatial structures of two images from same area at the contiguous time steps are identical, missing measurements can be estimated using predicted values from previous history. With this approach, it is possible to analyze a sequence of images as an on-line process.

In remote sensing data, the original distribution of the radiated intensity is modified by residual effects resulting from imperfect sensing of the target as well as atmospheric attenuation of the signal. Image reconstruction algorithms are based on the premise that a reasonable representation of the original image can be recovered from a blurred, noisy version of the true target scene. The effectiveness of the algorithms depends on the validity of the image model. Using a Bayesian estimation method, the system enhances pictorial information of the image data for better interpretation by increasing the discrimination capability for imagery that has been modified by the residual effects and atmospheric attenuation. The Bayesian method uses a statistical model that can represent a digital image process in remote sensing. The proposed system for adaptive reconstruction of sequential imagery involves simultaneous considerations of temporal trends in the process in conjunction with anisotropic spatial optical properties.

Of the various techniques that might be considered for the studies of vegetation processes, only satellite remote sensing offers a realistic possibility to obtain the requisite data because of the large aerial extent, strong spatial and temporal dynamics, and logistical inaccessibility of the vegetation. Reflectance data from Advanced Very High Resolution Radiometer (AVHRR) that is deployed on the NOAA-n series of polar orbiting meteorological satellites are obtainable globally on a daily basis. Analyses of the relations between AVHRR spectral measurements and vegetation related phenomena have been exceptionally successful and have encouraged great interest in the AVHRR sensor as a global vegetation observatory [3][4]. The multispectral reflectance data of AVHRR have been transformed and combined into various vegetation indices to minimize the variability due to external factors [5]. The most commonly used vegetation index is the normalized vegetation index (NVI) that is defined as the difference between AVHRR Channels 2 and 1 divided by their sum. It is well known that NVI is strongly dependent on the phenology

of vegetation. This study involves a temporal analysis of Korean Peninsula imagery. The NVI images were computed from the multispectral reflectance data that were compiled over Korean Peninsula by the AVHRR system and the proposed system was then applied to a temporal sequence of the NVI images.

This paper is organized as follows: Description of a statistical model that is assumed for the reconstruction is presented in Section II. Section III contains the algorithms of Bayesian restoration, mean intensity estimation, spatial parameter estimation, adaptive prediction and missing recovery as well as the integrated system. In Section IV, the results of applying the algorithms to the AVHRR data are reported. Conclusions are presented in Section V.

II. MATHEMATICAL MODEL FOR DIGITAL IMAGE

This study uses a mathematical model for digital image processing, that is valid for many physical processes in remote sensing data. Modification of the originally radiated intensity due to residual effects of imperfect sensing and atmospheric attenuation of the signal can be represented by a linear system. An image is spatially correlated by making the linear system act upon the distribution of the original intensity. Let $I_n = \{1, 2, \cdots, n\}$ be the index set of n pixels for a sample image. If the mean intensity, original intensity and observed intensity processes at time t are repectively

$$\mathrm{U}_t = \{U_{t,i},\ i \in I_n\},\quad \mathrm{X}_t = \{X_{t,i},\ i \in I_n\} \text{ and } \mathrm{Y}_t = \{Y_{t,i},\ i \in I_n\},$$

the following model is assumed for remtely sensed image processing:

$$\begin{aligned} Y_{t,i} &= \sum_{j \in I_n} S_{t,ij} X_{t,j} + \varepsilon_t \\ X_{t,i} &= U_{t,i} + \eta_{t,i} \end{aligned} \tag{1}$$

where at time t, $S_{t,ij}$ is a spatial coefficient associated with the ith and jth pixels, ε_t and $\eta_{t,i}$ are random variables related to the spatial noise and the ith pixel's temporal error. For mathematical simplicity, the spatial attributes are assumed to be homogeneous over the whole image space. If necessary, sub-scenes could be analyzed if homogeneity characteristics are only localized. Under this assumption, the spatial noise has an identical distribution and the spatial operator corresponds to a homogeneous linear system on the

whole target area. The temporal error is considered to be dependent only on its own pixel's signal. If an image has a periodic boundary and is acted upon by a homogeneous linear system, the spatial operator has a circular form. Without time index, the spatial operator is taken the form of

$$\mathrm{S} = \mathrm{circular}[\ S_k\ ]_n \equiv \begin{pmatrix} S_0 & S_1 & S_2 & \cdots & S_{n-1} \\ S_{n-1} & S_0 & S_1 & \cdots & S_{n-2} \\ \vdots & \vdots & \vdots & \ddots & \vdots \\ S_1 & S_2 & S_3 & \cdots & S_0 \end{pmatrix}. \tag{2}$$

Without loss of generality, the spatial noise and the temporal error are assumed to be distributed with Gaussian:

$$\varepsilon_t \sim \text{IID } N(0, \sigma_t^2) \text{ and } \eta_{t,i} \sim \text{IID } (0, \delta_{t,i}^2). \tag{3}$$

III. FEEDBACK SYSTEM OF ADAPTIVE RECONSTRUCTION

The feedback system combines five filters: Bayesian Intensity Restoration Filter (BIRF), Adaptive Polynomial Prediction Filter (APPF), Missing Measurement Recovery Filter (MMRF), Mean Intensity Estimation Filter (MIEF), Spatial Parameter Estimation Filter (SPEF). Time and pixel indices are omitted for the variables to simplify notation in this section, if it is not necessary.

A. BAYESIAN INTENSITY RESTORATION FILTER

If the probability structure of the process is known, the original intensity can be restored from the observed data using Bayesian criterion [6]. Given an observed process Y, the Bayesian approach is to find the maximum a posteriori (MAP) estimate of X from the mode of the posterior probability distribution, equivalently to maximize the log likelihood function:

$$L_f = \log_e P(\mathrm{X}|\mathrm{Y}) + \log_e P(\mathrm{X}).$$

Denote Σ and Γ as the covariance matrices of the observation and the original intensity of a sample image under Gaussian assumption of (3). If there is prior information about the distribution of the original intensity, the posterior probability of X conditioned on Y,

$$f(\mathrm{X}|\mathrm{Y}) \propto \exp[\ (\mathrm{Y}-\mathrm{SX})'\Sigma^{-1}(\mathrm{Y}-\mathrm{SX}) + (\mathrm{X}-\mathrm{U})'\Gamma^{-1}(\mathrm{X}-\mathrm{U})]\ .$$

Given the spatial coefficient matrix S, the mean intensity U, the covariance matrices Σ and Γ, the log likelihood equation is

$$(\Gamma^{-1} + \Sigma^{-1}S'S)X = \Sigma^{-1}S'Y + \Gamma^{-1}U \tag{4}$$

To solve directly the linear equation of (4), it is necessary to compute the inverse of the matrice that have a dimension corresponding to the number of the pixels. However, the correct inverse is hardly obtained because the matrix dimension is too large even for small images. Using an iterative approach similar to the point-Jacobian iteration method [7], the equation of (4) can be solved without computing the inverse of the large matrice. Using the mathematical model of (1), Σ and Γ are diagonal matrices of $n \times n$. If the spatial operator S is a circular matrix, the matrix $S^* = S'S = \text{circular}[\ S_k^*]_n$ is also a circular matrix as in (2). The left side of (4) can be restated:

$$(\Gamma^{-1} + \Sigma^{-1}S^*)X = D(I + D^{-1}C)X$$

where

$$D = \{D_{ij},\ i, j \in I_n\} \qquad \text{where } D_{ij} = \begin{cases} \dfrac{1}{\delta_i^2} + \dfrac{S_0^*}{\sigma^2} & \text{if } i = j \\ 0 & \text{if } i \neq j \end{cases}$$

$$C = \text{circular}[\ C_k]_n \qquad \text{where } C_k = \begin{cases} 0 & \text{if } k = 0 \\ \dfrac{S_k^*}{\sigma^2} & \text{if } k \neq 0 \end{cases}$$

The equation of (4) is then rewritten as an iterative form:

$$\hat{X}_k = W\ \hat{X}_{k-1} + Z, \quad k = 1, 2, \cdots \tag{5}$$

where

$$W = -D^{-1}C \text{ and } Z = (\Sigma D)^{-1}S'Y + (\Gamma D)^{-1}U.$$

It converges to an unique solution of X in (4) for a given initial $\hat{X}_0$ if W has a spectral radius less than 1. If the matrix S^* is diagonally dominant, that is,

$$\sum_{k \neq 0} |S_k^*| \leq |S_0^*|,$$

for each row of $W = \{w_{ij},\ i, j \in I_n\}$,

$$\sum_{j \in I_n} |w_{ij}| = \sum_{k=1}^{n-1} \left| \frac{S_k^*}{D_{ii}\sigma^2} \right| = \frac{\sum_{k=1}^{n-1} |S_k^*|}{\sigma^2/\delta_i^2 + |S_0^*|} < 1$$

and the spectral radius of W is then less than 1 [8]. In image processing, the residual effects from nearby pixels are generally not greater than the spectral reflectance received from the pointed nominal pixel. Therefore, S^* can be assumed to be diagollay dominant. It requires to compute only the inverses of the diagonal matrices D, Σ and Γ. The first part of (5) in the right side is re-expressed for computational purpose:

$$WX = \{-V_i/D_{ii}\} \text{ where } V = \{V_i\} = \begin{pmatrix} X_1 & X_2 & \cdots & X_n \\ X_2 & X_3 & \cdots & X_1 \\ \vdots & \vdots & \ddots & \vdots \\ X_n & X_1 & \cdots & X_{n-1} \end{pmatrix} \begin{pmatrix} C_0 \\ C_1 \\ \vdots \\ C_{n-1} \end{pmatrix} \tag{6}$$

In practice, a "spread window" for the residual effects is usually chosen with a low order and computation of (6) is then reduced according to the order of the window.

B. MEAN INTENSITY ESTIMATION FILTER

Most environmental studies presume that a "surface patch" in an earth scene is likely to be spatially continuous and cohesive. Therefore, pixels close together tend to have the same intensity or similar intensities. A Gibbs random field (GRF) [9] is used to represent the spatial dependency of the mean intensity process in neighboring pixels by probabilistically quantifying the spatial smoothness. In this study, a homogenous GRF with a periodic boundary is used as a measure to quantify the spatial continuity probabilistically.

It is natural that neighboring pixels with closer intensity levels have a higher probability of being of the same class. Using this idea, spatial smoothness can be quantified for the image process by a pair-potential that is a function of Euclidean distance between the mean intensities of the pixel pairs. A GRF related to a pair-clique system C_p can define a probability structure of the class configuration ω:

$$\begin{aligned} P(\omega) &= \varkappa_c^{-1} \exp[\ E_p(\omega)] \\ E_p(\omega) &= \sum_{(i,j)\in C_p} \alpha_{ij}[\ U(\omega_i) - U(\omega_j)]^{\ 2} \end{aligned} \tag{7}$$

where $\varkappa_c$ is a normalizing factor, α_{ij} is a nonnegative coefficient that represents a "bonding strength" of the ith and jth pixels, and $U(\omega_i)$ is the mean intensity of the

class ω_i of the ith pixel. In (7), the energy function E_p can be expressed with a function of U rather than ω:

$$E_p(\mathrm{U}) = \mathrm{U}'\mathrm{A}\mathrm{U}.$$

Consider a pair-clique system that is defined with the pixel pairs $\{(i,j)\colon i<j \text{ and } i,j\in I_n\}$. If the pair-clique system is related to a homogenous random field with a periodic boundary, $\mathrm{A} = \mathrm{circular}[A_k]_n$ is a circular matrix, in which

$$A_0 = 2\sum_{(i,j)\in C_p}\alpha_{(j-i)} \text{ and } A_k = \begin{cases} -\alpha_{(j-i)} & \text{if } k=j-i \text{ or } n-(j-i),\ (i,j)\in C_p \\ 0 & \text{otherwise} \end{cases} \tag{8}$$

where $\alpha_{(j-i)}$ is the coefficient associated with the index difference $(j-i)$ between two pixels. For example, for a sample image of $n=n_c\times n_r$ with the second order pair-clique system, the ith pixel has four neighbors with the indices j_k, $k=1,2,3,4$ where

$$j_k=\begin{cases} i+h_k & \text{if } i\le n-h_k \\ i+h_k-n, & \text{otherwise} \end{cases}$$

and $h_1=1$, $h_2=n_c-1$, $h_3=n_c$, $h_4=n_c+1$. Each pixel actually has eight neighbors in the second neighborhood system. However, it is redundant to consider the other four neighbors whose indices are less than the center pixel's because the pair system is symmetric. If α_k is the coefficient related to the index difference h_k, $A_0=2(\alpha_1+\alpha_2+\alpha_3+\alpha_4)$, $A_1=A_{n-1}=-\alpha_1$, $A_{n_c-1}=A_{n-n_c+1}=-\alpha_2$, $A_{n_c}=A_{n-n_c}=-\alpha_3$, $A_{n_c+1}=A_{n-n_c-1}=-\alpha_4$ and all the other circular elemements of A are zeros.

Given the covariance matrix Γ and the bonding coefficient matrix A, the posterior probability of the mean intensity conditioned on the original intensity is

$$f(\mathrm{U}|\mathrm{X})\propto\exp[\ (\mathrm{X}-\mathrm{U})'\Gamma^{-1}(\mathrm{X}-\mathrm{U})+\mathrm{U}'\mathrm{A}\mathrm{U}]$$

Using the Bayesian technique and the iterative method as in BIRF, the iteration equation of MIEF is established by redefining (5):

$$\hat{\mathrm{U}}_k = \mathrm{W}\ \hat{\mathrm{U}}_{k-1} + \mathrm{Z} = -\mathrm{D}^{-1}\mathrm{C}\ \hat{\mathrm{U}}_{k-1} + (\Gamma\mathrm{D})^{-1}\mathrm{X},\quad k=1,2,\cdots$$

where

$$\mathrm{D} = \{D_{ij},\ i, j \in I_n\} \qquad \text{where } D_{ij} = \begin{cases} \frac{1}{\delta_i^2} + A_0 & \text{if } i = j \\ 0 & \text{if } i \neq j \end{cases}$$

$$\mathrm{C} = \text{circular}[\ C_k\ ]_n \qquad \text{where } C_k = \begin{cases} 0 & \text{if } k = 0 \\ A_k & \text{if } k \neq 0 \end{cases}$$

For the bonding coefficient matrix of (8), it is shown that MIEF always converges to an unique solution of U. Larger choice for the bonding coefficient yields smoother estimation. It is not easy to determine the amount of smoothing in the image. Nevertheless, it is not necessary to consider this problem seriously in practice. Without knowing the true image, there is no globally ideal solution. Lee was estimated approximately the coefficients for some special cases [11].

C. SPATIAL PARAMETER ESTIMATION FILTER

For many remote sensing processes where temporal changes of atmospheric environment affect the spatial components, the spatial coefficients should be considered not to be stationary over time. Let X and Y be defined on a periodic Gaussian random field in a finite image space. The likelihood and its equations of the spatial components are

$$L_f \equiv \log_e f(\mathrm{S}, \Sigma | \mathrm{X}, \mathrm{Y}) \propto n \log_e \sigma^2 + \frac{1}{\sigma^2} (\mathrm{Y} - \mathrm{SX})'(\mathrm{Y} - \mathrm{SX}) \tag{9}$$

The product of S and X in (9) can be rewritten to take derivatives conveniently as in (6):

$$\mathrm{SX} = \mathrm{C}_x \mathrm{V}_s \text{ where } \mathrm{C}_x = \begin{pmatrix} X_1 & X_2 & \cdots & X_n \\ X_2 & X_3 & \cdots & X_1 \\ \vdots & \vdots & \ddots & \vdots \\ X_n & X_1 & \cdots & X_{n-1} \end{pmatrix} \text{ and } \mathrm{V}_s = \begin{pmatrix} S_0 \\ S_1 \\ \vdots \\ S_{n-1} \end{pmatrix}.$$

The vector V_s corresponds to the discrete location-invariant point spread function of the original intensity process. For the low order spread function, the column dimension of C_x are greatly reduced by eliminating zero elements of V_s. The maximum likelihood estimates are then obtained by taking the partial derivatives with respect to V_s and σ^2 in (9):

$$\hat{\mathrm{V}}_s = (\mathrm{C}_x' \mathrm{C}_x)^{-1} \mathrm{C}_x' \mathrm{Y} \text{ and } \hat{\sigma}^2 = \frac{(\mathrm{Y} - \mathrm{C}_x \hat{\mathrm{V}}_s)'(\mathrm{Y} - \mathrm{C}_x \hat{\mathrm{V}}_s)}{n}.$$

D. ADAPTIVE POLYNOMIAL PREDICTION FILTER

Original uncontaminated intensity, one characteristic of the physical processes that have been remotely sensed and displayed in the image, exhibits temporal variations about the mean intensity that is assumed to be due only to the target characteristics that are generally dependent only on the target site. The temporal variations may be represented by autoregressive moving average time serieses. This assumption is proper for a stationary process. However, most physical processes observed in remote sensing data usually exhibit systematic trends in properties over a long time. This type of variation is most apparent in the mean intensity process and usually dominates the temporal process.

The variation in the mean intensity can be adaptively tracked by using a polynomial function of time. If a realization of the intensity is sequentially given, the prediction of the mean intensity at next time step can reflect more recent variations in the process with an exponential weight criterion. If the original intensity process is only signal-dependent, it can be assumed that the process is spatially independent. Under this assumption, the mean intensity process can be considered for each pixel separately. Using a polynomial model of order p, the original intensity process at time t in a pixel is represented by

$$X_t = g_p(t) + \eta_t \text{ where } U_t = g_p(t) = \theta_{t,0} + \sum_{k=1}^{p} \theta_{t,k} t^k. \tag{10}$$

If the process is consistent with (10) and $\{x_\tau,\ \tau = t_1, t_2, \cdots, t_m\}$ is a realization sequence of the mean intensity from the origin $t_0 = 0$, the prediction of the original intensity at time t, $\hat{U}_t$ can be estimated with the exponentially weighted least squares criterion:

$$\min \left\{ \eta^2_{t_m} + \sum_{j=1}^{m-1} \lambda^{(t_{j+1}-t_j)} \eta^2_{t_j} \right\} \tag{11}$$

where λ is a weight coefficient selected in the range of $0 < \lambda \leq 1$. The adaptive polynomial filter sequentially generates the estimate with the exponentially weighted least squares criterion by adaptively updating the polynomial coefficients over time:

$$\text{for } m > p \text{ and } t > t_m, \quad \hat{U}_t = \Theta_m' \mathrm{T} \tag{12}$$

where

$$\Theta_m = \begin{pmatrix} \phi_0(t_m) & \phi_1(t_m) & \cdots & \phi_p(t_m) \\ \phi_1(t_m) & \phi_2(t_m) & \cdots & \phi_{p+1}(t_m) \\ \vdots & \vdots & \ddots & \vdots \\ \phi_p(t_m) & \phi_{p+1}(t_m) & \cdots & \phi_{2p}(t_m) \end{pmatrix} \begin{pmatrix} \psi_0(t_m) \\ \psi_1(t_m) \\ \vdots \\ \psi_p(t_m) \end{pmatrix}$$

$$\mathrm{T} = (1 \quad t \quad t^2 \quad \cdots \quad t^p)'$$

For $j \geq 1$,

$$\begin{aligned} \phi_k(t_j) &= \lambda^{t_j - t_{j-1}} \phi_k(t_{j-1}) + t_j^k, \quad k = 0, 1, 2, \cdots, 2p \\ \psi_k(t_j) &= \lambda^{t_j - t_{j-1}} \psi_k(t_{j-1}) + t_j^k x_{t_j}, \quad k = 0, 1, 2, \cdots, p \end{aligned} \tag{13}$$

where $\phi_k(t_0) = \psi_k(t_0) = 0, \ \forall k$. The adaptive polynomial filter requires $p+1$ variables for ψ_k of (13) for each pixel respectively. Therefore, the memory complexity makes it desirable to utilize the lowest order model that adequately captures the variations for the purpose of locally tracking the temporal trend in recent observations.

The temporal error variance can be directly estimated with the predicted values, but it results in the abnormal estimation if the measurement is incorrectly observed by imperfect sensing at that time. Using a weight for the adjustment according to the temporal variation, the variance of X_t is smoothly updated over time:

$$\delta_t^2 = \beta_s \delta_{t-1}^2 + (1 - \beta_s)(x_t - \hat{U}_t)^2$$

where $0 \leq \beta_s \leq 1$.

E. MISSING MEASUREMENT RECOVERY FILTER AND INTEGRATED SYSTEM

Given the original intensity, missing measurements can be estimated directly from the first equation of (1) by assuming that the spatial structures are same in the contiguous time steps for MMRF. The feedback system combines the five filters for the adaptive reconstruction of sequential imagery. The predicted mean intensity in APPF is an estimate of the original intensity of (1). If the system is initiated, APPF provides the estimate to MMRF for recovering missing measurements, MIEF for estimating the current mean intensity process and BIRF for initiating the filter. Using the current observation and the recovered data in MMRF, SPEF calculates the spatial parameters, that are provided to BIRF as a component of the probability structure of the original intensity for the Bayesian restoration as well as the mean intensity estimated in MIEF. BIRF restores the original intensity based on the Bayesian criterion and the polynomial coefficients in APPF are updated using the original intensity reconstructed in BIRF.

In the integrated system, the mean intensity is estimated using the predicted values, the image is reconstructed based on the estimated mean intensity and the reconstructed image is used for next prediction. Due to this recursive estimation, APPF is often too slow to

follow the trend correctly and extreme observations may result in the divergence of the estimated process. It is necessary for the mean intensity prediction to be more sensitive to changes in observations and reasonably compatible with the observed data. Though the measurements are spatially contaminated by the residual effects, they should still have the same or a very similar trend as that of the original intensity process. If a pixel currently has an observation, APPF estimates the pixel's intensity by fitting the observation at the present time. This makes the estimate compatible with the observation while reflecting the temporal trend. For this purpose, APPF of (12) is modified:

$$\hat{U}_t = \begin{cases} \hat{\Theta}_m{}'\mathrm{T}, & \text{if } y_t \text{ exists} \\ \Theta_m{}'\mathrm{T}, & \text{otherwise} \end{cases}$$

where

$$\hat{\Theta}_m = \begin{pmatrix} \hat{\phi}_0(t_m) & \hat{\phi}_1(t_m) & \cdots & \hat{\phi}_p(t_m) \\ \hat{\phi}_1(t_m) & \hat{\phi}_2(t_m) & \cdots & \hat{\phi}_{p+1}(t_m) \\ \vdots & \vdots & \ddots & \vdots \\ \hat{\phi}_p(t_m) & \hat{\phi}_{p+1}(t_m) & \cdots & \hat{\phi}_{2p}(t_m) \end{pmatrix} \begin{pmatrix} \hat{\psi}_0(t_m) \\ \hat{\psi}_1(t_m) \\ \vdots \\ \hat{\psi}_p(t_m) \end{pmatrix}$$

$$\hat{\phi}_k(t_m) = \lambda^{t-t_m}\phi_k(t_m) + t^k, \quad k = 0,1,2,\cdots,2p$$
$$\hat{\psi}_k(t_m) = \lambda^{t-t_m}\psi_k(t_m) + t^k y_t, \quad k = 0,1,2,\cdots,p$$

The feedback system is outlined in Figure 1.

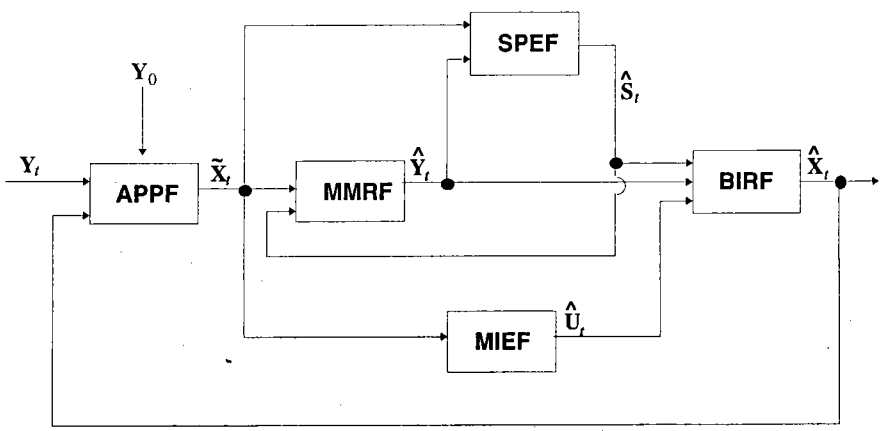

Figure 1. Outline of Adaptive Feedback System

IV. APPLICATIONS

The 600×1000 AVHRR image data analyzed in this study were acquired over Korean Peninsula from February to November of 1991. First, the 16 images of NVI data were generated from the Local Average Cover (LAC) data set, the highest resolution available from AVHRR with approximately $1\ km^2$ spatial resolution, that is geographically registered. The proposed system is originally designed to analyze sequential imagery of a high temporal resolution as an on-line process by adaptively reconstructing the missing or contaminated data. However, the data source of Korean Peninsula imagery with a high temporal resolution was not available for this study, although AVHRR provides daily images of all regions of the globe. In order to show a temporal change for vegetation activity on Korean Peninsula using remotely sensed image data, the data set with the low temporal resolution were analyzed for the examples of this study instead of another data set with a high temporal resolution. Figure 2 contain the four of the 16 NVI images. Water areas, that are not of interest, were masked for the analysis. In the image illustrations, black shades on the land represent areas of missing measurement, and areas of higher NVI value have brighter shades. The sensor system failed to collect the observations mainly due to cloud cover at the observed date and the peculiar line as in the third illustration was generated by sensor noises. The upper part of the second image was blurred and some areas in the third and fourth images have unsmoothed shades. It might have resulted from atmospheric contamination or the presence of haze.

Because information from the current observation at each time step is gradually reflected in the estimation, the adaptive system may be suitable for the analysis of a image sequence of high temporal resolution for the on-line process. However, it often occurs that the data availability for the analysis is restricted by many reasons in practice. If the sequential imagery has a low temporal resolution, it may be reconstructed by combining the results that are generated by analyzing the sequence of the images in forward and backward time directions respectively. The exponential weight of (11) in the adaptive prediction indicates the desired trade-off between conflicting goals of fidelity with observations and temporal smoothness. The estimated process tends to be consistent with the temporal trend by using a weight close to 1, while it follows recent variation in the image space with a smaller weight. For the iterative approach of a low temporal resolution sequence, it is desirable to make the estimates rely more on the current observations.

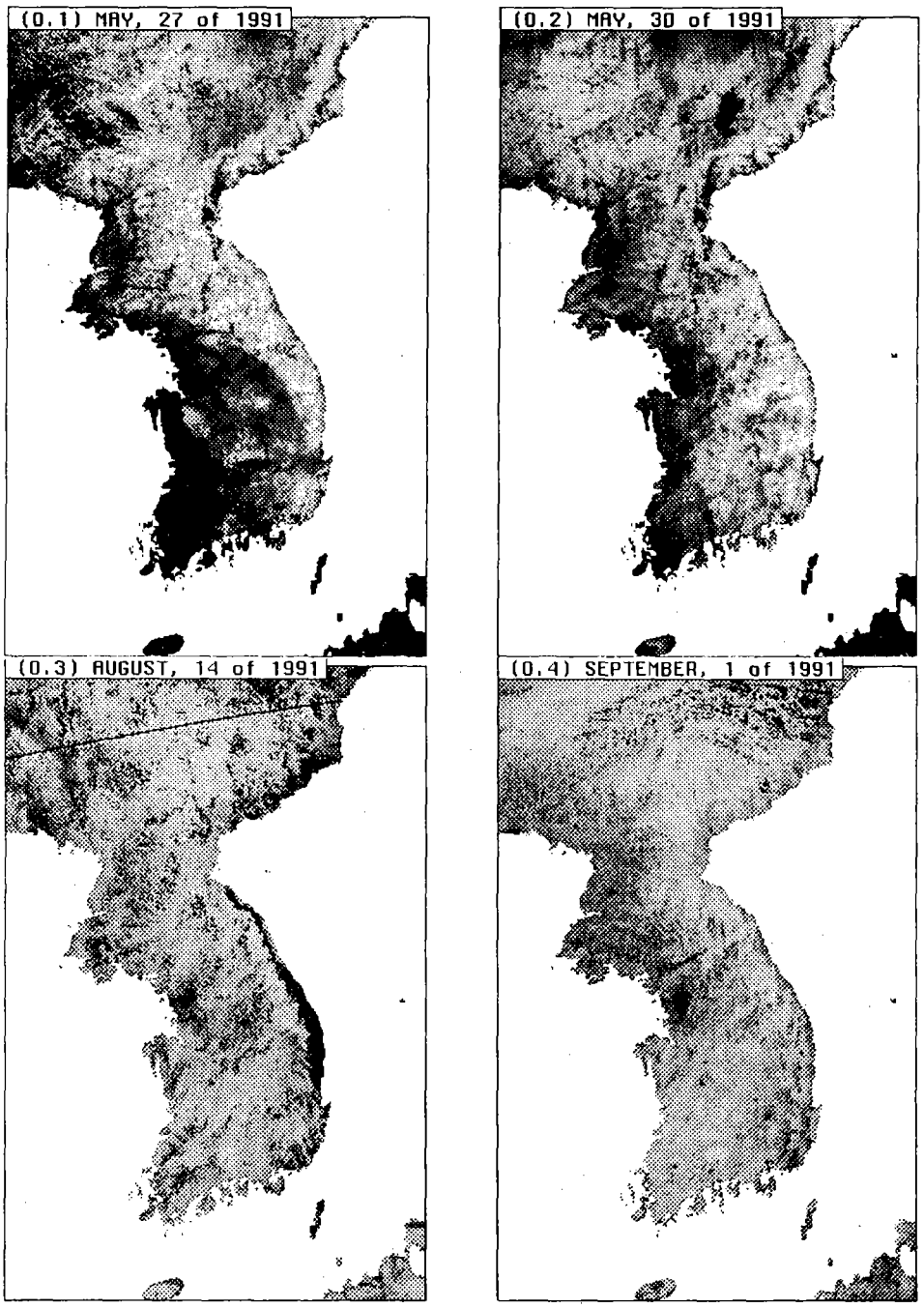

Figure 2. AVHRR NVI Images of 600×1000 Observed from Korean Peninsula in 1991 (black shade - missing, bright shade - high NVI, dark shade - low NVI)

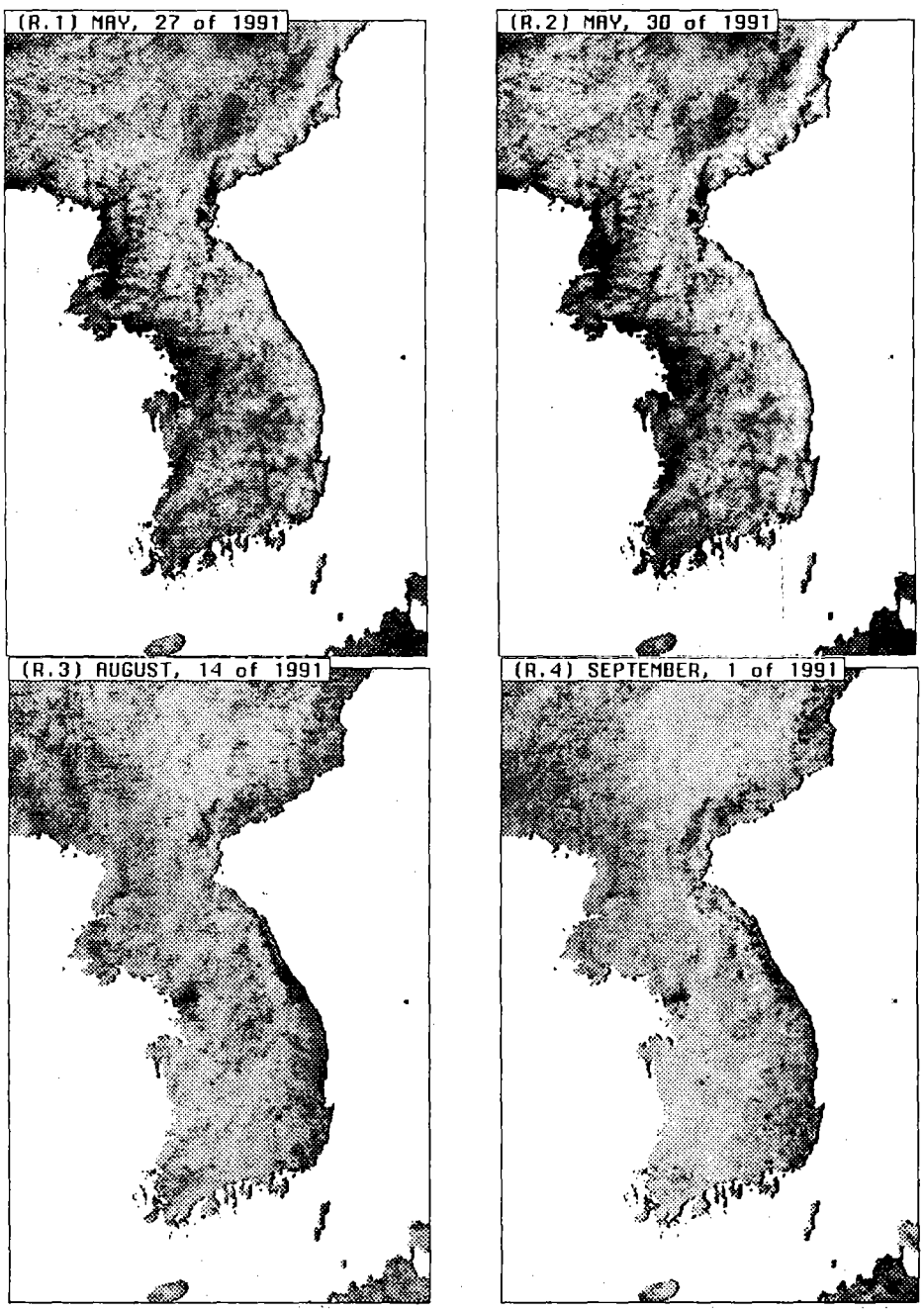

Figure 3. Reconstruction Results of Korean Peninsula NVI Images

The system was designed to set $\lambda = 0.95$ using the second order polynomial function and the anisotropic spatial operator corresponding to 5×5 spread window. An initial sequence of three images is required to initiate the system. Under the assumption that the process is periodic, the initial sequence was calculated based on the first and the last images by recovering missing measurements with the observations of the spatially-nearest pixels if they exist. Figure 3 illustrates the reconstructed images corresponding to Figure 2. The results were obtained by averaging the estimated values in both time directions using the adaptive system with same condition.

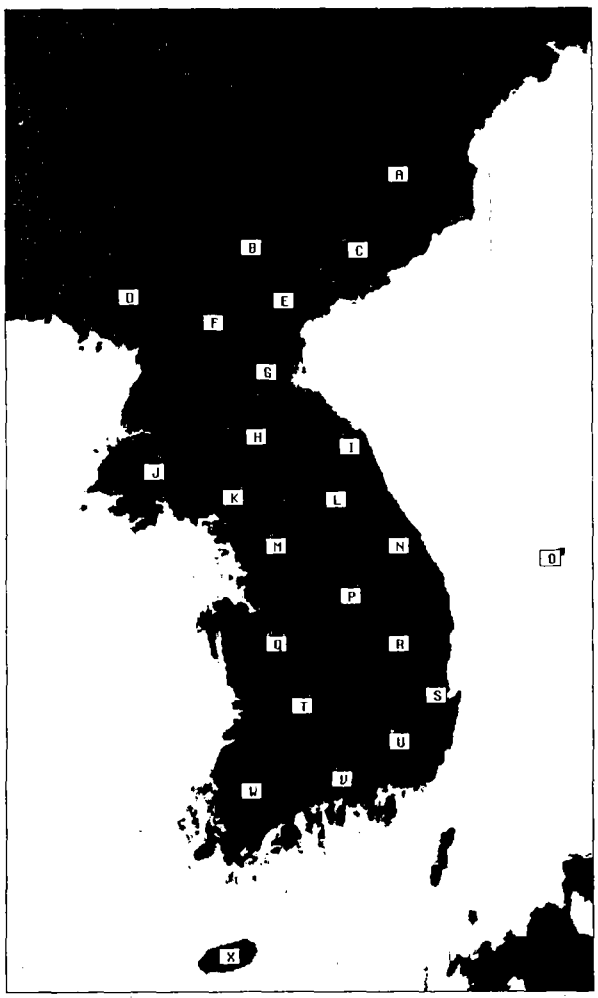

Figure 4. Location Map of Points Chosen for Plots of NVI Values

Figure 5 and 6 plot the observed and reconstructed spectral responses over time for 24 points, which were chosen arbitrarily, but uniformly over the entire peninsula. Figure 4 shows locations of the chosen points. In the plots of Figure 5 and 6, the values of each point were calculated by averaging the spectral responses except missing data from the square area of 3 x 3 pixels. If all the measurements of 9 pixels are missing, the point was assigned to zero. The short term variations exhibited in the observed data are not due to real changes in the land cover response. They mainly result from sensor's imperfect characteristics and environmental interference. For example, if an area is partially covered by clouds, it is observed with low NVI values.

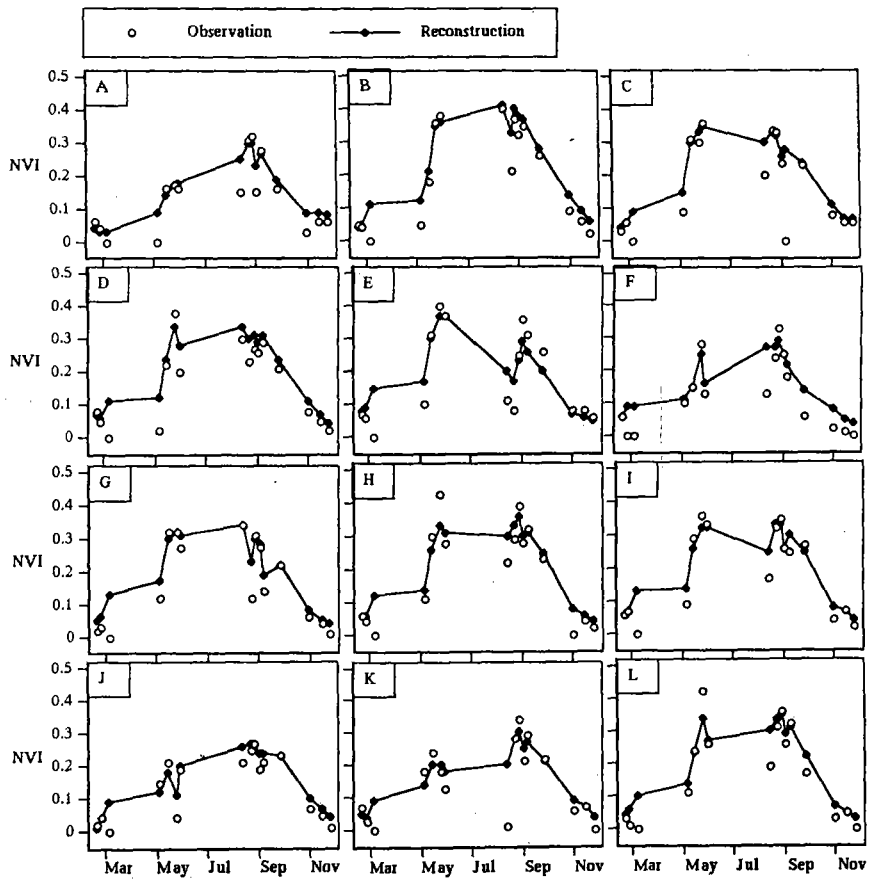

Figure 5. Plots of NVI Values for Observed and Reconstructed Series (missing points are assigned to zero values)

The variations in the process have been stabilized according to the local temporal trend in the reconstructed series. The plots show that the adaptive system recovers deteriorated responses of low values in high vegetation season as well as missing data with plausible estimates by compromising between observation and local trend. It is necessary that the field study of relations between timely ground truth and remotely-sensed NVI measurements precede the quantitative analysis of the reconstruction results. At the present time, the ground truth information associated with NVI values in Korean Peninsula is very limited. Therefore, the detailed analysis of quantitative evaluation for the results will be left for another study including the examination of NVI processes in the peninsula.

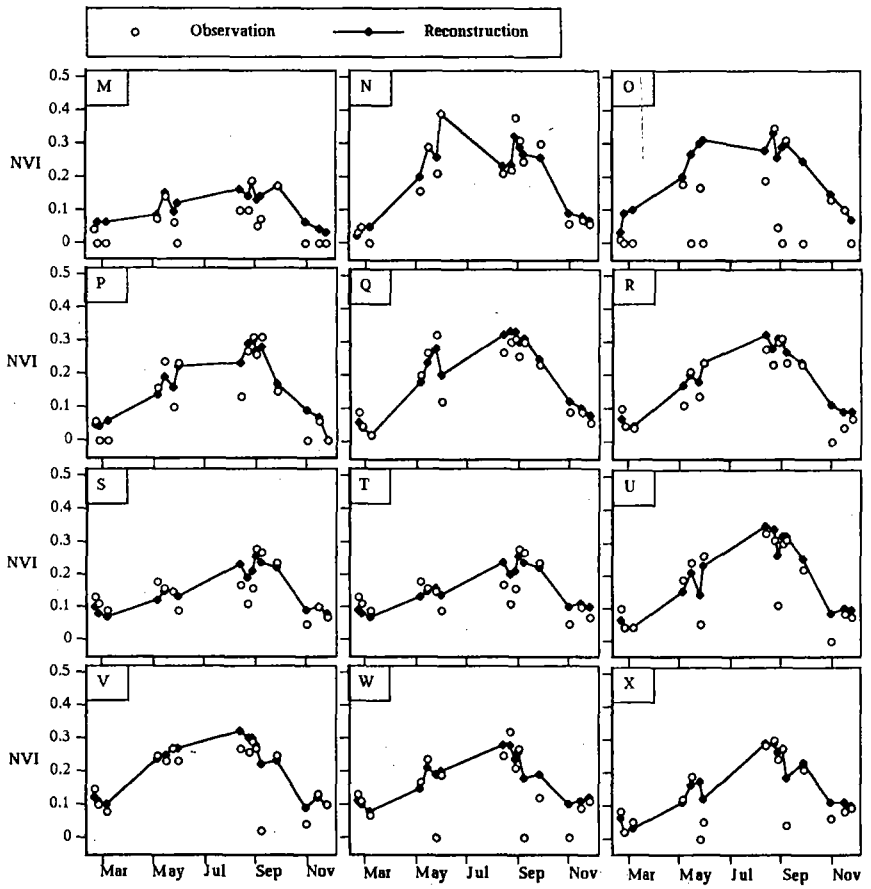

Figure 6. Plots of NVI Values for Observed and Reconstructed Series

V. CONCLUSIONS

Accomplishing multitemporal analyses is complicated by numerous intervening factors, such as instrument calibration, view geometry, atmospheric attenuation and cloud occurrence, that tend to obscure the relation between ground and satellite observed spectral measurements. Temporal resolution is mostly reduced by cloud occurrence and sensor noise. For many locations on the globe, cloud occurrence prevents regularly repeating ground measurements. Even if the magnitude of the cloud impact in reducing temporal resolution varies significantly in time and space, on any given day, approximately 50% of the earth's surface are obscured by clouds. The problem of cloud occurrence can be to great extent avoided through the use of the adaptive system, that is designed as an automatic on-line process to analyze a sequence of images acquired at shorter time intervals. This technique increases the discrimination capability for imagery that has been modified by spatial properties of imperfect sensing on the target and atmospheric attenuation of the signal as well as the recovery capability for missing measurements. The adaptive system may lead to improved classification of imagery and more correct detection of temporal changes.

The proposed system was applied for a sporadic series of 16 AVHRR images collected over Korean Peninsula for one year and the final estimation of the series was obtained by combining the results of the analyses in different time directions. As shown in the experimental results, temporal trends in vegetation changes are exposed more clearly in the reconstructed series than the observations, and most of missing/deteriorated measurements are typically recovered successfully by the system. However, for the on-line process, the adaptive system requires sequential data observed at short time intervals such that it smoothly tracks temporal changes of the process through transient periods in the forward time direction. In near future, the experimental study for the adaptive reconstruction system will be extended using AVHRR images that have been collected over Korean Peninsula on a daily basis.

ACKNOWLEDGMENT

We acknowledge the support of the department of Oceanography in Seoul National University and Professor Kyu Sung Lee in Inha University, who provided he AVHRR data set of Korean Peninsula for this research.

REFERENCES

[1] S. Lee and M.M. Crawford, "An adaptive reconstruction system for spatially corre lated multispectral multitemporal images," *IEEE Trans. Geosci. Remote Sens.*, Vol. 29, 1991, pp494-508.

[2] B.N. Holben, "Characteristics of maximum value composite image from temporal AVHRR data," *Int. J. Remote Sens.*, Vol. 7, 1986, pp1417-1434.

[3] J.R.G. Townsend and C.J. Tucker, "Objective assessment of AVHRR data for land cover mapping," *Int. J. Remote Sens.*, Vol. 5, 1984, pp492-501.

[4] W.R. Philipson and W.L. Teng, "Operational interpretation of AVHRR vegetation indices for world crop information," *Photogramm. Eng. Remote Sens.*, Vol. 54, 1988, pp55-59

[5] J.D., Tarpley, S.R.Schneider and R.L. Money, "Global vegetation indices from the NOAA-7 meteorological satellite," *J. Climate Appl. Meteorol.*, Vol. 23 , 1984, pp491-494.

[6] H.C. Andrews, *Introduction to Mathematical Techniques inPattern Recognition*, Wiley Interscience, New York, 1972.

[7] R.S. Varga, *Matrix Iterative Analysis*, Prentice-Hall Inc., 1962.

[8] C.G. Cullen, *Matrix and Linear Transformation*, Addison-Wesley Publishing Company, 1972.

[9] H.O. Georgii, *Canonical Gibbs Measure*, Springer-Verlag, Berlin, 1979.

[10] H. Derin and H. Elliott, "Modelling and segmentation of noisy and relaxation algorithms for segmenting noncausal Markov random fields," *IEEE Trans. Pattern Anal. Machine Intell.*, Vol. 9, pp39-55, 1987.

[11] S. Lee, *An unsupervised hierarchical clustering image segmentation and an adaptive image reconstruction system for remote sensing*, Ph. D. Dissertation, Univ. of Texas at Austin, 1990.